JOC Article

Diversity-Oriented Synthesis of Privileged Benzopyranyl Heterocycles from *s-cis*-Enones

Heeseon An,† Sung-Jin Eum,† Minseob Koh,† Sung Kwang Lee,‡ and Seung Bum Park*,†

Department of Chemistry, Seoul National University, Seoul, 151-747, Korea, and Bioinformatics & Molecular Design Research Center, Seoul, 120-749, Korea

sbpark@snu.ac.kr

Received October 10, 2007

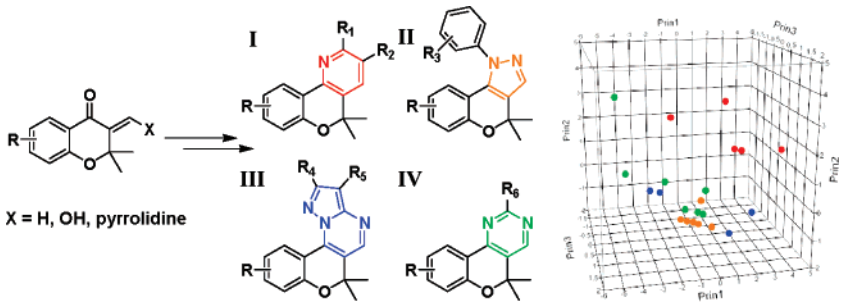

A novel strategy for the construction of benzopyranyl heterocyclic series with maximized diversity in the polar surface area on rigid scaffolds has been developed through a divergent synthetic pathway with high efficiency. *s-cis*-Enones embedded in a benzopyran skeleton were identified as versatile key intermediates for the synthesis of four different heterocycle libraries fused with a benzopyran substructure. These four novel core skeletons were designed by a creative recombination of the privileged skeletons: benzopyran, pyridine, pyrazole, pyrazolopyrimidine, and pyrimidine. The regioselective synthesis of each core skeleton was achieved by the introduction of three *s-cis* enone intermediates. This paper also explores the regioselective formation of arylpyrazole through the condensation of β-keto aldehyde with arylhydrazine under three different conditions and presents the mechanistic information that was obtained from the regioisomeric ratio of arylpyrazole based on the substituent's electronic effect and reaction temperature. It appears that the regioselective synthesis of arylpyrazole was achieved through the intriguing interplay of the nucleophilicity on arylhydrazine and the electrophilicity on dielectrophiles.

Introduction

In the postgenomic era, the systematic perturbation of complex biological processes with small-molecule probes has been in the spotlight in the field of chemical biology due to their potential applications as therapeutic agents and research tools in biology.[1] The essential elements in chemical biology are efficiency in biological evaluation with specific targets and the accessibility of small-molecule libraries to diverse core skeletons.[2] Therefore, the development of new synthetic routes for the construction of natural product-like small-molecule libraries with structural complexity, diversity, and various physicochemical properties is attracting attention from the scientific community involved in chemical biology and drug discovery.[3]

Diversity-oriented synthesis (DOS), which aims to populate the chemical space with skeletally and stereochemically diverse small molecules with high appending potentials, has been proven to be an essential tool for the discovery of bioactive small molecules.[4] The incorporation of privileged substructural motifs—a concept that there exist preferred molecular scaffolds that can provide ligands for diverse receptors, first introduced by Evans and co-workers in 1988—has become an essential element in DOS pathways.[5,6] Recently, our group reported the construction

† Seoul National University.
‡ Bioinformatics & Molecular Design Research Center.

(1) Schreiber, S. L. *Bioorg. Med. Chem.* **1998**, *6*, 1127−1152.
(2) Min, J.; Kim, Y. K.; Cipriani, P. G.; Kang, M.; Khersonsky, S. M.; Walsh, D. P.; Lee, J-Y.; Niessen, S.; Yates, J. R., III; Gunsalus, K.; Piano, F.; Chang, Y-T. *Nat. Chem. Biol.* **2006**, *3*, 55−59.
(3) (a) Schreiber, S. L. *Science* **2000**, *287*, 1964−1969. (b) Burke, M. D.; Schreiber, S. L. *Angew. Chem., Int. Ed.* **2004**, *43*, 46−58.
(4) (a) Koehler, A. N.; Shamji, A. F.; Schreiber, S. L. *J. Am. Chem. Soc.* **2003**, *125*, 8420−8421. (b) Nesterenko, V.; Putt, K. S.; Hergenrother, P. J. *J. Am. Chem. Soc.* **2003**, *125*, 14672−14673.

10.1021/jo702196f CCC: $40.75
Published on Web 02/12/2008

of 22 discrete and novel core skeletons embedded with a privileged benzopyran substructure through a branching DOS strategy. We emphasized the maximization of skeletal diversity in a 3-D space, and we confirmed the importance of the core skeletons by illustrating dramatic differences in the biological activities of compounds sharing the same appendices but having different 3-D structures.[7]

We are currently focusing on the importance of diversity in polar surface area for the synthesis of diverse bioactive molecules. Small molecules having different polar surface areas on rigid scaffolds might induce various interactions such as hydrogen bonding and electrostatic and dipole−dipole interactions, which are one of the main types of noncovalent forces involved in receptor−ligand binding. Furthermore, a survey of the relevant literature reveals that heterocyclic compounds having differently oriented heteroatoms demonstrate a variety of biological activities.[8] For example, nitrogen-containing heterocycles such as pyridine[8a−d], pyrazole[8e−i], pyrazolopyrimidine[8j−m], and pyrimidine[8n−o] are frequently observed structural moieties in many bioactive molecules targeting HIV-1 reverse transcriptase,[8c] angiotensin II receptor,[8e] COX-2,[8h] factor Xa,[8i] corticotropin-releasing factor (CRF),[8j,k,n] $GABA_A$ receptor,[8l] etc. Therefore, developing a new strategy for an efficient synthesis of diverse heterocyclic compounds having distinct orientations of the heteroatoms could be important. After considering all these facts, we initiated a rational design and pathway development for a benzopyranyl heterocycle library. In this paper, we would like to introduce a divergent synthetic pathway to combine various heterocycles with a benzopyran substructure (Figure 1A). Our divergent synthetic pathway was achieved by the identification of *s-cis* enones (**2**, **4**, and **10**) as the versatile key intermediates that can be transformed into drug-like 5-, 6-, and [5 + 6]-membered heterocyclic scaffolds: pyridine, pyrazole, pyrazolopyrimidine, and pyrimidine. We selected these heterocycles not only because they are observed in biologically active natural products but also because of their interesting feature, the distinct orientation of heteroatoms, particularly nitrogen, on a (poly)aromatic rigid core skeleton. As shown in Figure 1B, the electrostatic potentials and electron density of the four novel skeletons were calculated to confirm that these compounds were sufficiently diverse in terms of polar surface area; the novel core skeletons have almost identical shapes in the 3-D space confirmed by the alignment of energy-minimized conformers, but the electrostatic potentials on the rigid core skeletons are relatively different as shown in isosurface diagram.

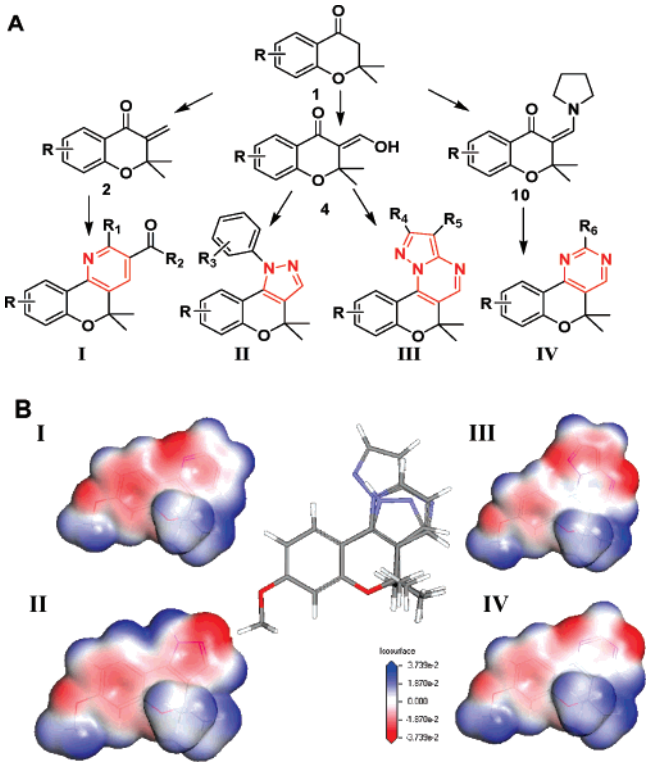

FIGURE 1. (A) An overall synthetic scheme for four unique heterocyclic core skeletons (**I**−**IV**) via the direct fusion of a privileged benzopyran motif with the heterocycles (pyridine (**I**), pyrazole (**II**), pyrazolopyrimidine (**III**), and pyrimidine (**IV**)). (B) The emphasis on the 3-D structural similarity in the four discrete core skeletons through the alignment of energy-minimized conformers and the discrepancy in the distribution of polar surface area among the core skeletons **I**−**IV**. The most stable conformer was selected from a set of conformers generated by diverse conformation generation protocol which was implemented in Discovery Studio 1.7 (Accelrys Software, Inc.). The four different conformers from each core skeleton were superimposed with a methoxyaryl moiety on benzopyrans. The polar surface area is illustrated by an isosurface diagram (isovalue is set as 0.017 C) after an electrostatic potential and electron density calculation. All of the calculations were performed using the Materials Studio 4.2 program. A generalized gradient approximation (GAA) for the exchange-correlation function of Perdew, Burke, and Ernzerhof (PBE) was used with the double-numerical basis set with polarization (DNP) as implemented in DMol3.

(5) Nicolaou, K. C.; Pfefferkorn, J. A.; Roecker, A. J.; Cao, G.-Q.; Barluenga, S.; Mitchell, H. J. *J. Am. Chem. Soc.* **2000**, *122*, 9939−9953.

(6) (a) Evans, B. E.; Rittle, K. E.; Bock, M. G.; DiPardo, R. M.; Freidinger, R. M.; Whitter, W. L.; Lundell, G. F.; Veber, D. F.; Anderson, P. S.; Chang, R. S. L.; Lotti, V. J.; Cerino, D. J.; Chen, T. B.; Kling, P. J.; Kunkel, K. A.; Springer, J. P.; Hirshfield, J. *J. Med. Chem.* **1988**, *31*, 2235−2246. (b) DeSimone, R. W.; Currie, K. S.; Mitchell, S. A.; Darrow, J. W.; Pippin, D. A. *Comb. Chem. High Throughput Screening* **2004**, *7*, 473−493.

(7) Ko, S. K.; Jang, H. J.; Kim, E.; Park, S. B. *Chem. Commun.* **2006**, *28*, 2962−2964.

(8) (a) Pinder, A. R. *Nat. Prod. Rep*. **1992**, *1*, 17−23. (b) Plunkett, A. O. *Nat. Prod. Rep*. **1992**, *1*, 581−590. (c) Genin, M. J.; Poel, T. J.; Yagi, Y.; Biles, C.; Althaus, I.; Keiser, B. J.; Kopta, L. A.; Friis, J. M.; Reusser, F.; Adams, W. J.; Olmstead, R. A.; Voorman, R. L.; Thomas, R. C.; Romero, D. L. *J. Med. Chem*. **1996**, *39*, 5267−5275. (d) Nkansah, P. A.; Haines, A. H.; Stamford, N. P. J. *Chem. Commun*. **2003**, *6*, 784−785. (e) Almansa, C.; Gomez, L. A.; Cavalcanti, F. L.; de Arriba, A. F.; Garcia-Rafanell, J.; Forn, J. *J. Med. Chem*. **1997**, *40*, 547−558. (f) Pargellis, C.; Tong, L.; Churchill, L.; Cirillo, P.; Gilmore, G.; Graham, A. G.; Grob, P. A.; Hickey, E. R.; Moss, N.; Pav, S.; Regan, J. *Nature Struct. Biol.* **2002**, *9*, 268−272. (g) Sakya, S. M.; DeMello, K. M. L.; Minich, M. L.; Rast, B.; Shavnya, A.; Rafka, R. J.; Koss, D. A.; Cheng, H.; Li, J.; Jaynes, B. H.; Ziegler, C. B.; Mann, D. W.; Petras, C. F.; Seibel, S. B.; Silvia, A. M.; George, D. M.; Lund, L. A.; St. Denis, S.; Hickman, A.; Haven, M. L.; Lynch, M. P. *Bioorg. Med. Chem. Lett*. **2006**, *16*, 288−292 (h) Singh, S. K.; Vobbalareddy, S.; Shivaramakrishna, S.; Krishnamraju, A.; Rajjak, S. A.; Casturi, S. R.; Akhilab, V.; Raoa, Y. K. *Bioorg. Med. Chem. Lett*. **2004**, *14*, 1683−1688. (i) Qiao, J. X.; Cheng, X.; Smallheer, J. M.; Galemmo, R. A.; Drummond, S.; Pinto, D. J. P.; Cheney, D. L.; He, K.; Wong, P. C.; Luettgen, J. M.; Knabb, R. M.; Wexler, R. R.; Lam, P. Y. S. *Bioorg. Med. Chem. Lett*. **2007**, *17*, 1432−1437. (j) Huang, C. Q.; Wilcoxen, K. M.; Grigoriadis, D. E.; McCarthy, J. R.; Chen, C. *Bioorg. Med. Chem. Lett*. **2004**, *14*, 3943−3947. (k) Chen, C.; Wilcoxen, K. M.; Huang, C. Q.; Xie, Y.-F.; McCarthy, J. R.; Webb, T. R.; Zhu, Y.-F.; Saunders, J.; Liu, X.-J.; Chen, T.-K.; Bozigian, H.; Grigoriadis, D. E. *J. Med. Chem*. **2004**, *47*, 4787−4798. (l) Selleri, S.; Bruni, F.; Costagli, C.; Costanzo, A.; Guerrini, G.; Ciciani, G.; Gratteri, P.; Besnard, F.; Costa, B.; Montali, M.; Martini, C.; Fohlin, J.; De Siena, G.; Aiello, P. M. *J. Med. Chem*. **2005**, *48*, 6756−6760. (m) Selleri, S; Gratteri, P.; Costagli, C.; Bonaccini, C.; Costanzo, A.; Melani, F.; Guerrini, G.; Ciciani, G.; Costa, B.; Spinetti, F.; Martinib, C.; Brunia, F. *Bioorg. Med. Chem*. **2005**, *13*, 4821−4834. (n) McCluskey, A.; Keller, P. A.; Morgan, J.; Garner, J. *Org. Biomol. Chem.* **2003**, *1*, 3353−3361. (o) Prekupec, S.; Makuc, D.; Plavec, J.; Suman, L.; Kralj, M.; Pavelic, K.; Balzarini, J.; De Clercq, E.; Mintas, M.; Raic-Malic, S. *J. Med. Chem*. **2007**, *50*, 3037−3045.

SCHEME 1. General Procedure for the Synthesis of Benzopyranylpyridine Core Skeletons via Hantzsch Condensation

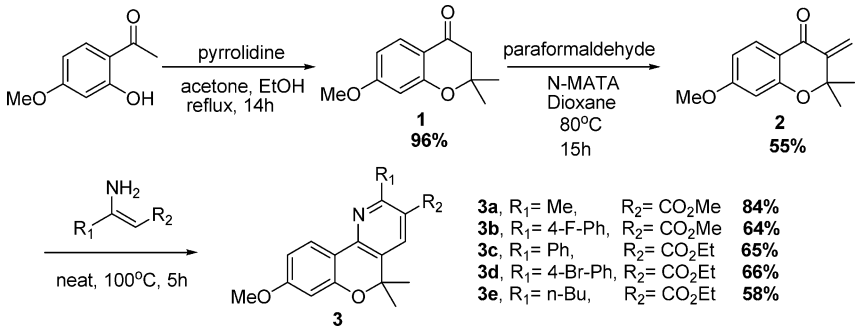

Accordingly, this difference might induce diverse interactions with various biological targets. Therefore, benzopyranyl compounds fused with various such heterocycles might have a high potential as small-molecule modulators or bioprobes for biomedical research because of their diverse orientation of heteroatoms and polar surface area.

Results and Discussion

Synthesis of Benzopyranyl Pyridines (I). For the synthesis of pyridine-fused benzopyran core skeleton **3**, we first synthesized 3-methylenechromen-4-one **2** as a versatile starting material by the aldol condensation of dihydrochromen-4-one **1** with formaldehyde in the presence of *N*-methylanilinium trifluoroacetate (*N*-MATA). The resulting α,*β*-unsaturated ketone **2** was transformed into a 2,3,5,6-tetrasubstituted pyridine moiety via Hantzsch condensation followed by the spontaneous dehydrogenation of 1,4-dihydropyridine.[9] The best result was obtained when the reaction was performed under neat conditions compared to in protic or aprotic solvents, probably because of the short life-times of carbanions generated from enamines. The enamino esters were synthesized from *β*-keto esters reacting with NH_4OAc (5 equiv) under a refluxing condition in MeOH for 5 h.[10] It turned out that enaminoesters synthesized from *β*-keto esters are good substrates for the synthesis of desired pyridine-fused benzopyran core skeletons via Hantzsch condensation with excellent to reasonable yields (Scheme 1). Furthermore, the general scope of this reaction was tested with different electron withdrawing groups—cyano and amide—at the R_2 position, and the desired products were obtained under identical reaction conditions in relatively low yields.

Synthesis of Benzopyranylpyrazoles (II). In our initial attempt toward the synthesis of the pyrazole-fused benzopyran core skeleton **II**, 3-methylenechromen-4-one **2** was treated with arylhydrazine under refluxing ethanol conditions. However, intermediate **2** was transformed into a complex mixture of regioisomers and unknown byproducts that might have been caused mainly by the incomplete aromatization of the intermediate pyrazoline.[11] When the pyrazole synthesis using α,*β*-unsaturated ketone **2** failed to provide the desired product in high yield, we focused on routes through a hydroxy-substituted *s-cis* enone **4** because 3-hydroxymethylenechromen-4-one **4** could be tautomerized to *β*-keto aldehyde **5** under the reaction condition; therefore, the resulting intermediate **5** could efficiently interact with arylhydrazine nucleophile, which turned out to be a key step for an efficient transformation to the desired pyrazole-ring system with complete aromatization.[12] As shown in Table 1, two regioisomers were obtained in our initial attempt, and interestingly, we observed systematic patterns of the regioisomeric ratio during the reaction optimization for the regioselective synthesis of pyrazole-fused benzopyran core skeleton **II** from

TABLE 1. Regioisomeric Ratio in the Synthesis of Benzopyranylarylpyrazole from *β*-Keto Aldehyde 5 with Arylhydrazines under Three Different Reaction Conditions

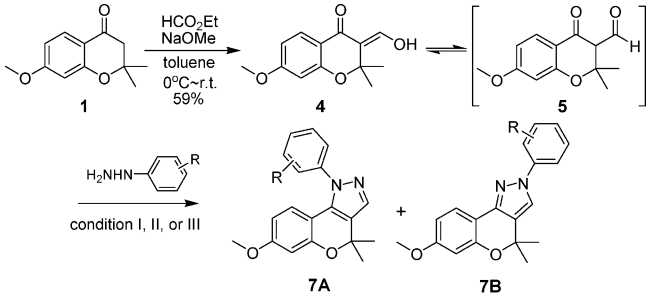

Condition I: $ArNHNH_2 \cdot HCl$, TEA, EtOH, 78°C, within 5 h;
Condition II: $ArNHNH_2 \cdot HCl$, EtOH, 78°C, within 5 h;
Condition III: $ArNHNH_2 \cdot HCl$, acetic acid/MeOH, 30 °C, within 1 h.

entry	R	I (A/B)[b]	II (A/B)[b]	III (A/B)	yield of I[a] (%)	yield of III[a] (%)
7a	4-MeO	85:15	60:40	*f*	80	*f*
7b	4-Me	88:12	60:40	93:7	87	92
7c	4-H	97:3	74:26	96:4	77	96
7d	4-F	97:3	75:25	96:4	80	95
7e	4-Cl	92:8	83:17	97:3	75	96
7f	4-CF_3	>99:1[d]	94:6	98:2	88[c]	97
7g	4-NO_2	*e*	100:0	100:0	84[c]	95

[a] Isolated yields of major product **7A** under the given conditions unless otherwise mentioned. [b] Isomer ratio determined by ^1H NMR spectroscopy of crude products. [c] Isolated yield of major products synthesized under condition II. [d] Regioisomeric ratio was measured by ^1H NMR after 24 h of reaction time under condition I. [e] The reaction was not completed in 48 h, and intermediate **6A** was the major component in the crude mixture according to the crude NMR. See the Supporting Information. [f] Data was not obtained due to the instability of 4-methoxyphenylhydrazine under the given conditions.

(9) (a) Sobolev, A.; Franssen, M. C. R.; Vigante, B.; Cekavicus, B.; Zhalubovskis, R.; Kooijman, H.; Spek, A. L.; Dubur, G.; Groot, A. *J. Org. Chem.* **2002**, *67*, 401−410. (b) Eisner, U.; Kuthan, J. *Chem. Rev.* **1972**, *72*, 1−42 and references therein. (c) Sagitullina, G. P.; Glizdinskaya, L. V.; Sagitullin, R. S. *Chem. Heterocycl. Compd.* **2002**, *38*, 1336−1341. (d) Wang, L-M.; Sheng, J.; Zhang, L.; Han, J-W.; Fan, Z-Y.; Tian, H.; Qian, C-T. *Tetrahedron* **2005**, *61*, 1539−1543. (e) Dagnino, L.; Li-Kwong-Ken, C. M.; Wolowyk, M. W.; Wynn, H.; Triggle, C. R.; Knaus, E. E. *J. Med. Chem.* **1986**, *29*, 2524−2529.

(10) Hsiao, Y.; Rivera, N. R.; Rosner, T.; Krska, S. W.; Njolito, E.; Wang, F.; Sun, Y.; Armstrong, J. D., III; Grabowski, E. J. J.; Tillyer, R. D.; Spindler, F.; Malan, C. *J. Am. Chem. Soc.* **2004**, *126*, 9918−9919.

(11) Huang, Y. R.; Katzenellenbogen, J. A. *Org. Lett.* **2000**, *2*, 2833−2836.

(12) (a) May, D.A., Jr.; Lash, T. D. *J. Org. Chem.* **1992**, *57*, 4820−4828. (b) Meegalla, S. K.; Doller, D.; Liu, R.; Sha, D.; Soll, R. M.; Hanoa, D. S. *Tetrahedron Lett.* **2002**, *43*, 8639−8642.

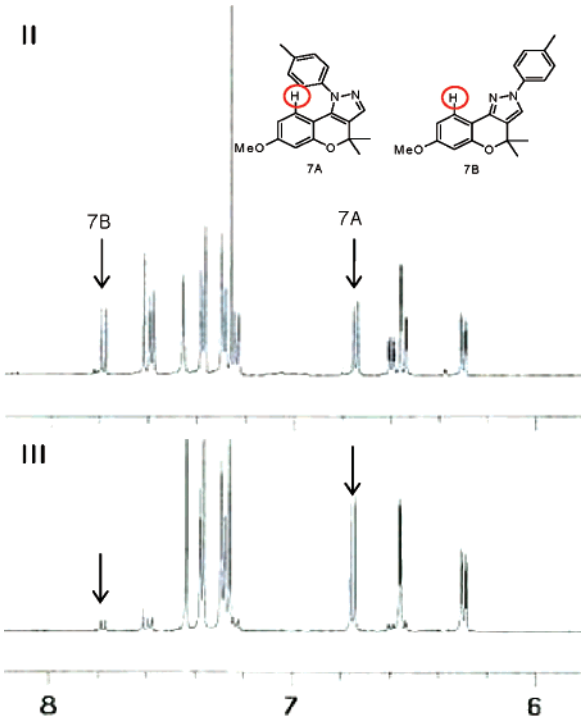

FIGURE 2. Crude ^{1}H NMR spectra of arylpyrazoles. The ratio of regioisomers (**7A** and **7B**) was determined by the simple integration of the crude ^{1}H NMR spectra of arylpyrazole **7b** under conditions II and III without any further purification.

β-keto aldehyde **5**. The desired arylpyrazoles were synthesized from **4** and arylhydrazines having various substituents under three different conditions: the condensation of **4** with arylhydrazines in the neutral salt-free form by the treatment of triethylamine (condition I), the same reaction with arylhydrazines in the hydrochloride salt form (condition II), and the condensation of **4** with arylhydrazines in aqueous acetic acid (condition III). Subsequently, the regioisomeric ratios of **7A** and **7B** were measured by ^{1}H NMR spectroscopy, shown in Figure 2 as the typical crude ^{1}H NMR spectra of arylpyrazoles **7b**. In the case of **7A**, a significant upfield shift of proton at a meta position to a methoxy group was observed; this suggests that this proton is shielded by the 1-aryl substituent that might be perpendicular to the major plane of the molecule, as indicated in the previous literature.[13] Therefore, the regioisomeric ratio of **7A** and **7B** was measured by integrating the characteristic signals in the crude ^{1}H NMR spectra. The structure of the desired arylpyrazole was confirmed by 1-D ^{1}H nuclear Overhauser effect (NOE) difference spectra (see the Supporting Information).

Mechanistic Studies on the Regioselectivity in Arylpyrazole Synthesis. With the desired regioselectivity of arylpyrazole in hand, we turned our attention to the next challenge—the mechanistic understanding of regioselectivity in arylpyrazole synthesis through the condensation of β-keto aldehyde with arylhydrazine. The regioselective synthesis of a pyrazole moiety has been a challenge; however, only a few papers have suggested mechanistic pathways related to the reactions between dielectrophiles and arylhydrazine.[11,14] In fact, many different reaction conditions were reported to have produced the desired regioisomers of arylpyrazole in high yields without a proper rationalization of their regioisomeric outcomes.[14−16] In light of this discrepancy in the literature, we pursued the mechanistic rationalization of the regioselectivity on the arylpyrazole synthesis through the interplay of arylhydrazine with hydroxy-substituted *s-cis* enone **4**. It is generally accepted in the literature that the aldehyde moiety has better electrophilicity in the β-keto aldehyde **5** that is a tautomer of **4**.[12] When we treated **1** with phenylhydrazine under reaction condition that was identical to the that employed during the pyrazole synthesis, we did not observe any hydrazone formation on cyclic ketone. Therefore, it was hypothesized that the regioisomeric ratio in the pyrazole synthesis might result from the competition between two plausible reaction pathways: One is the reaction between the aldehyde of **5** and the terminal nitrogen of arylhydrazine, and the other is the reaction between aldehyde of **5** and the internal nitrogen. As shown in Table 1, our investigation revealed that the internal nitrogen of arylhydrazine is more likely to form an enamine with aldehyde in a hydrochloride salt form (condition II) than in a neutral form (condition I), which is caused by the reduced nucleophilicity of the terminal nitrogen in arylhydrazine due to the protonation with hydrochloride. In the absence of the hydrochloride salt in the case of entries **7f** and **7g**, however, we observed a significant reduction in the reaction rate or no formation of a pyrazole moiety; this led us to conclude that the hydrochloride in the salt of arylhydrazine enhanced the pyrazole transformation by acid catalysis on the cyclic ketones after the formation of the enamines and also controlled the nucleophilicity of the two nitrogens in arylhydrazine. When the condensation of arylhydrazine with **4** was performed in the presence of aqueous acetic acid (condition III), we observed a significant enhancement in the regioselectivity and reaction yield during the arylpyrazole synthesis that might have occurred because of the catalytic effect of acetic acid on the condensation phase. An interesting correlation between the regioselectivity and electronic factor was observed, i.e., the regioselectivity for the arylpyrazole synthesis increased with the electronic effects of the substituents on arylhydrazine.

At this stage, we carried out another series of reactions by changing the reaction conditions to investigate more about the reaction mechanism (see Table 2). The completion time of this reaction reduced as the temperature was increased; however,

(13) Gabbutt, C. D.; Hepworth, J. D.; Heron, B. M.; Coles, S. J.; Hursthouse, M. B. *J. Chem. Soc., Perkin Trans. 1* **2000**, *17*, 2930−2938.

(14) Reference that showed best regioselectivity on arylpyrazole synthesis under condition I: Singh, S. K.; Reddy, M. S.; Shivaramakrishna, S.; Kavitha, D.; Vasudev, R.; Babu, J. M.; Sivalakshmidevi, A.; Rao, Y. K. *Tetrahedron Lett.* **2004**, *45*, 7679−7682.

(15) References that showed the best regioselectivity on arylpyrazole synthesis under condition II: (a) Penning, T. D.; Talley, J. J.; Bertenshaw, S. R.; Carter, J. S.; Collins, P. W.; Docter, S.; Graneto, M. J.; Lee, L. F.; Malecha, J. W.; Miyashiro, J. M.; Rogers, R. S.; Rogier, D. J.; Yu, S. S.; Anderson, G. D.; Burton, E. G.; Cogburn, J. N.; Gregory, S. A.; Koboldt, C. M.; Perkins, W. E.; Seibert, K.; Veenhuizen, A. W.; Zhang, Y. Y.; Isakson, P. C. *J. Med. Chem.* **1997**, *40*, 1347−1365. (b) Primofiore, G.; Marini, A. M.; Settimo, F. D.; Salerno, S.; Bertini, D.; Via, L. D.; Magno, S. M. *J. Heterocycl. Chem.* **2003**, *40*, 783−788. (c) Chetoni, F.; Settimo, F. D.; Motta, C. L.; Primofiore, G. *J. Heterocycl. Chem.* **1993**, *30*, 1653−1658. (d) Campagna, F.; Palluotto, F.; Carotti, A.; Maciocco, E. *Farmaco* **2004**, *59*, 849−856. (e) Habeeb, A. G.; Praveen Rao, P. N.; Knaus, E. E. *J. Med. Chem.* **2001**, *44*, 3039−3042. (f) Press, J. B.; Birnberg, G. H. *J. Heterocycl. Chem.* **1985**, *22*, 561−564.

(16) References that showed no clear differences on regioselectivity between condition I and II: (a) Regan, J.; Breitfelder, S.; Cirillo, P.; Gilmore, T.; Graham, A. G.; Hickey, E.; Klaus, B.; Madwed, J.; Moriak, M.; Moss, N.; Pargellis, C.; Pav, S.; Proto, A.; Swinamer, A.; Tong, L.; Torcellini, C. *J. Med. Chem.* **2002**, *45*, 2994−3008. (b) Bagley, M. C.; Davis, T.; Dix, M. C.; Widdowson, C. S.; Kipling, D. *Org. Biomol. Chem.* **2006**, *4*, 4158−4164.

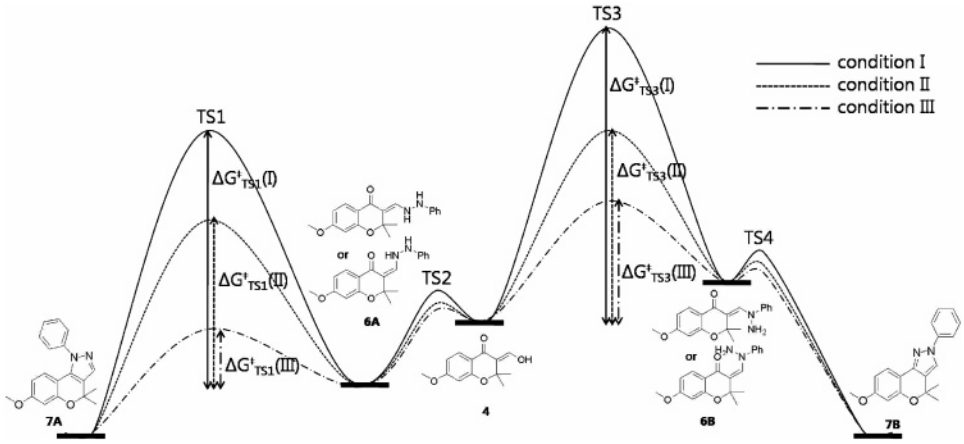

FIGURE 3. Proposed energy diagram for arylpyrazole synthesis.

TABLE 2. Regioisomeric Ratio in the Synthesis of Arylpyrazole 7c under Different Reaction Temperatures

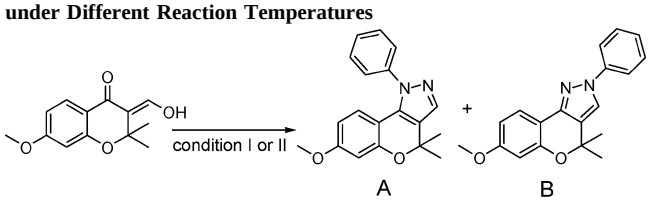

Condition I: $PhNHNH_2 \cdot HCl$, TEA; Condition II: $PhNHNH_2 \cdot HCl$
[a]Reaction was not completed in 48 h

T (°C)	solvent	time (h)	**I** (**A**/**B**)	**II** (**A**/**B**)
30	EtOH	>48	*a*	*a*
40	EtOH	48	72:28	62:38
50	EtOH	24	82:18	71:29
60	EtOH	12	95:5	77:23
80	EtOH	5	97:3	74:26
100	i-PrOH	5	>99:1	54:46

[a] Reaction was not completed in 48 h.

conditions I and II caused a drastic difference in the temperature-dependent regioselectivity. Under condition I (phenylhydrazine in the neutral form), the regioselectivity improved as the temperature was increased. On the other hand, in the case of condition II (phenylhydrazine in the hydrochloride salt form), the regioselectivity enhanced up to 77/23 (**A**/**B**) at 60 °C, and then it deteriorated back to approximately 1/1 at 100 °C (see Table 2). In the case of condition III, we did not observe the temperature-dependent regioisomeric ratio, because the arylpyrazole synthesis under condition III was completed within 1 h even at 30 °C with excellent regioselectivity.

After considering all of the factors, an energy diagram for the arylpyrazole synthesis was proposed with two discrete reaction pathways in a simplified version that led to two regioisomers (**7A** and **7B**) through two plausible intermediates (**6A** and **6B**) via four transition states (TS1−4), as shown in Figure 3. The rate-determining steps were different for the two reaction pathways. The condensation of enamine **6A** was probably the rate-determining step for the synthesis of **7A** via the nucleophilic attack of the internal nitrogen on cyclic ketone. In contrast, the rate-determining step for the synthesis of **7B** was the formation of enamine **6B** from **4** with less nucleophilic internal nitrogen on arylhydrazine. Initially, we focused on the relative nucleophilicity of the internal vs external nitrogens of arylhydrazine as well as the neutral vs hydrochloride salt form. As shown in Table 1, the electronic effect of the substituent on arylhydrazine influences the nucleophilicity of the two nitrogens on arylhydrazine, which was demonstrated by the direct correlation of electrodeficiency on arylhydrazine with the regioselectivity. However, the acid-catalyzed activation of the electrophiles (aldehyde or cyclic ketone) can also significantly influence the reaction route for the synthesis of the two regioisomers. The regioisomeric ratio was influenced by the activation energy change resulting from the acid catalysis through the activation of the electrophiles. Therefore, the activation energies, $\Delta G^{\ddagger}_{TS1}$(II) and $\Delta G^{\ddagger}_{TS3}$(II), for the rate-determining steps under condition II were less as compared to $\Delta G^{\ddagger}_{TS1}$(I) and $\Delta G^{\ddagger}_{TS3}$(I) for the rate-determining steps under condition I due to the acid catalysis by the hydrochloride salt. With aqueous acetic acid acting as a solvent under condition III, the activation energies, $\Delta G^{\ddagger}_{TS1}$(III) and $\Delta G^{\ddagger}_{TS3}$(III), were sufficiently decreased due to the acid catalysis on carbonyl moieties, which leads to the completion of the arylpyrazole synthesis within 30 min at 30 °C with excellent regioselectivity. This excellent regioselectivity can be rationalized as follows: The favored equilibrium of **4** with **6A** allowed an enriched population of **6A** in the reaction mixture, and $\Delta G^{\ddagger}_{TS1}$(III) was considerably less than $\Delta G^{\ddagger}_{TS3}$(III). Under condition I, we proposed that the activation energy of the transition state for **7A**, $\Delta G^{\ddagger}_{TS1}$(I), was less than that for **7B**, $\Delta G^{\ddagger}_{TS3}$(I), and the complete conversion to arylpyrazole proceeded rather slowly because of the absence of an acid catalyst. At the low reaction temperature under condition I, **6A** was dominant in the reaction mixture, confirmed by the crude NMR (entry **7g** in Table 1 and Supporting Information), but the activation energy barrier was quite high in both directions, and an extended reaction time was required for the completion of the reaction; this allows a chance to produce the other regioisomer **7B**. As the temperature was increased from 40 to 100 °C, the dominant intermediate **6A** could yield **7A**, which improved the regioselectivity from 72:28 to >99:1 (**7A**/**7B**). Under condition II, the hydrochloride salts reduce the nucleophilicity of arylhydrazine and enhance the reaction rate by the activation of the electrophiles (aldehyde for TS3 or cyclic ketone for TS1). The activation energy difference of $\Delta G^{\ddagger}_{TS1}$(II) and $\Delta G^{\ddagger}_{TS3}$(II) under condition II might be less than that under condition I because the highest regioisomeric ratio was 77:23. The regioisomeric ratio reached the maximum at 60 °C and then reduced to 1:1 at 100 °C because the thermal energy offered by the system was high enough for the two reaction pathways to be nonselective.

SCHEME 2. General Procedure for the Synthesis of Pyrazolo[1,5-*a*]pyrimidine-Fused Benzopyran Core Skeletons

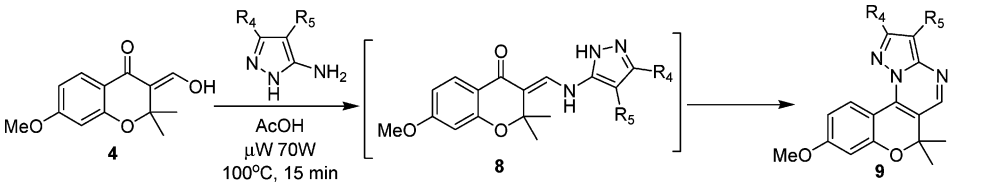

SCHEME 3. General Procedure for the Synthesis of Benzopyranylpyrimidine Core Skeletons[a]

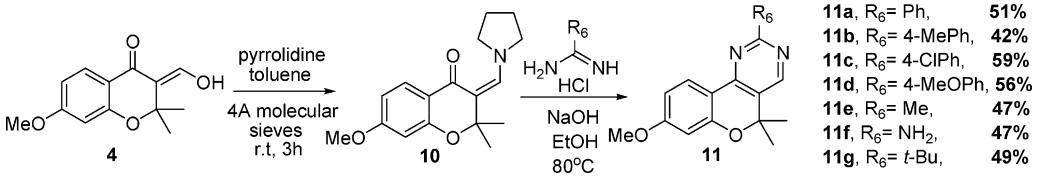

[a] The yield of the final products was obtained over a two-step procedure.

Synthesis of Benzopyranylpyrazolo[1,5-*a*]pyrimidines (III). Having proposed the mechanistic rationalization of regioselectivity in arylpyrazole synthesis, we next successfully accomplished a synthesis of pyrazolo[1,5-*a*]pyrimidine core structures from the hydroxy-substituted *s-cis* enone **4** by treatment with 3-aminopyrazole derivatives. Our earlier attempts afforded only an enamine intermediate **8** without any of the desired product under reaction conditions similar to those used for the pyrazole formation. After an extensive screening of the reaction conditions, the desired pyrazolo[1,5-*a*]pyrimidine-fused benzopyran core skeleton **9** was synthesized in excellent yields as a single regioisomer under microwave irradiation (70 W, 100 °C) for 15 min in glacial acetic acid (Scheme 2). The successful synthesis of pyrazolo[1,5-*a*]pyrimidine opens up the possibility for the application of this system to other [5 + 6]-membered polycycles using dinucleophiles.

Synthesis of Benzopyranylpyrimidines (IV). Finally, the synthesis of the pyrimidine moiety was accomplished by the introduction of new *s-cis* enone intermediate **10**. When the previous intermediates **2** and **4** were tested for this transformation, we only obtained complex mixtures from **2** and retro-aldol product from **4** without any enamine formation, which is an essential step for the following cyclization. Therefore, we attempted a detour, performing not the imine formation directly from *β*-keto aldehyde but the transamination of amidine through an enaminone intermediate **10** as well, which is in situ generated by the treatment of the hydroxy-substituted *s-cis* enone **4** with stoichiometric amounts of pyrrolidine. To our satisfaction, this hypothesis turned out to be correct. The facilitation of amine−amidine exchange can smoothly transform the enaminone **10** to the desired pyrimidine-fused benzopyran core skeleton **11** in relatively high yields (Scheme 3). The instability of **10** induces an equilibrium shift back to 3-hydroxymethylenechromen-4-one **4**, which undergoes a retro-aldol reaction in this reaction condition; this is the major cause for the medium to acceptable yields. However, the transamination−cyclization step from isolated **10** to **11** itself has excellent yields, and yet the isolation yield of **10** is relatively low (data not shown). Our attempt to address this issue by generating a stable enaminone using other amines such as piperidine, morpholine, and DMAP did not afford any improvements.

Chemoinformatic Visualization of Molecular Diversity on Four Unique Core Skeletons (I−IV). To visualize the diversity in the polar surface area, a diversity matrix, which includes all members of the representative compounds, was developed on the basis of nine molecular descriptors using PreADME (BMD, Seoul, Korea) and illustrated with three principal components (PCs) calculated using JMP (SAS Institute, Inc., Cary, NC). In Figure 4, the score plot is a result of performed principle components analysis (PCA) as the diagnostic tool in the similarity/diversity analysis of molecular descriptors. From unbiased calculations, it was observed that the four different core skeletons were distributed differently in the 3-D chemical space of calculated three principal components PC1, PC2, and PC3 explaining together 90.2% of the total variance in molecular descriptors. PC1 factor, which explains 55.7% of the variance, is mainly constituted by molecular weight (MW), van der Waals (VDW) surface area,[17a] number of rotatable bonds, hydrophobic VDW surface area, and calculated log *P* (AlogP98)[17b] (see the Supporting Information for PC loading values). PC2 factor, which explains 25.2% of the variance, is influenced by polar VDW surface area and the H-bond donor/acceptor VDW surface area.[17c] PC3 factor, accounting for 9.3% of the variance, includes number of rings and H-bond donor surface area. PC2 and -3 could effectively differentiate each core skeleton by the polar surface area and number of rings, and PC1 identified the diversity within the same class of core skeletons by size and lipophilic descriptors.

Conclusion

By virtue of the rich chemistry of the *s-cis* enone system, the key intermediate can be subjected to various synthetic transformations that lead to four discrete and drug-like core skeletons. To emphasize the importance of the diverse charge distributions in the DOS pathways, we designed and synthesized benzopyran-embedded small molecules merged with diverse heterocycles having distinct orientations of the polar surface

(17) (a) Labute, P. *J. Mol. Graphics, Mod.* **2000**, *18*, 464−477. (b) Ghose, A. K.; Viswanadhan, V. N.; Wendoloski, J. J. *J. Phys. Chem. A* **1998**, *102*, 3762−3772. (c) Bush, B. L.; Sheridan, R. P. *J. Chem. Inf. Comput. Sci.* **1993**, *33*, 756−762.

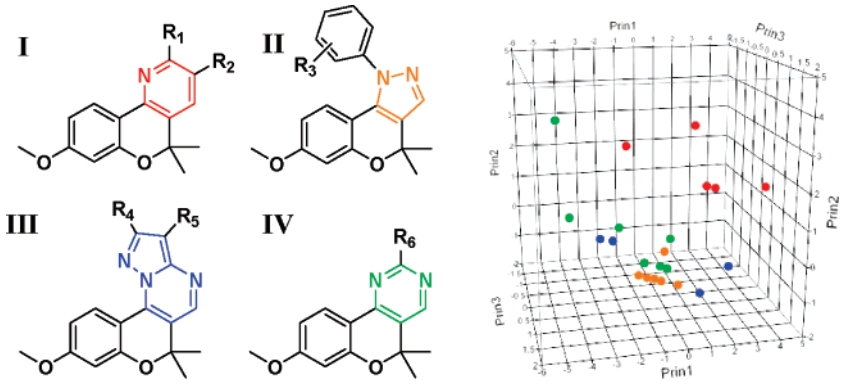

FIGURE 4. Principal component analysis of the benzopyranyl heterocyclic core skeletons **I**−**IV**, differently color-coded for visualization.

area. The efficient and regioselective synthesis of each core skeleton was achieved by the introduction of three *s-cis* enone intermediates: 3-methylenechromen-4-one **2**, 3-hydroxymethylenechromen-4-one **4**, and 3-pyrrolidinylmethylenechromen-4-one **10**. We could improve the efficiency of each transformation by lowering the key transition states: (1) the synthesis of pyrazole and pyrazolopyrimidine through the imine formation of the β-keto aldehyde **4** with the dinucleophiles, and not through the Michael addition of the α,β-unsaturated ketone **2**, and (2) the synthesis of pyrimidine through the transamination of amidine with the enaminone **10**, and not by the imine formation of amidine directly with the β-keto aldehyde **4**. In addition, we also explored the regioselective formation of arylpyrazole through the condensation of β-keto aldehyde with arylhydrazine under three different conditions and presented the mechanistic information that was obtained from the regioisomeric ratio of arylpyrazole based on the substituent's electronic effect and reaction temperature. It appears that the regioselective synthesis of arylpyrazole was achieved through the intriguing interplay of the nucleophilicity on arylhydrazine and the electrophilicity on dielectrophiles. These four novel core skeletons were designed by a creative recombination of the privileged skeletons: benzopyran, pyridine, pyrazole, pyrazolopyrimidine, and pyrimidine. We have a high expectation that these compounds could have quite different biological functions due to the diversity in their polar surface area, which might become a new diversity element for DOS. The biological evaluation results and the complete realization of a library with these novel core skeletons will be reported in due course.

Experimental Section

7-Methoxy-2,2-dimethyl-2,3-dihydrochromen-4-one (1). To a solution of 2-hydroxy-4-methoxyacetophenone (1.0 g, 6.02 mmol) and acetone (4.44 mL, 60.2 mmol) in ethanol (30 mL) was added pyrrolidine (1.51 mL, 18.06 mmol) in one portion. The mixture was heated to reflux for 14 h. After reaction completion monitored by TLC, the solvent was removed under reduced pressure. The resultant was diluted by EtOAc and washed with aqueous NH_4Cl (two times) solution and brine. The organic layer was dried over anhydrous $MgSO_4$ and filtered. Then, the filtrate was condensed under reduced pressure, and the resulting mixture was purified with silica gel flash column chromatography (EtOAc/hexanes = 1:20) to provide a desired product **1** (1.19 g, 96.0%) as a light yellow solid: TLC R_f = 0.42 (EtOAc/hexanes, 1:5); ^{1}H NMR (500 MHz, $CDCl_3$) δ 7.79 (d, J = 9.0 Hz, 1H), 6.54 (dd, J = 9.0, 2.5 Hz, 1H), 6.37 (d, J = 2.0 Hz, 1H), 3.83 (s, 3H), 2.67 (s, 2H), 1.61 (s, 6H); ^{13}C NMR (125 MHz, $CDCl_3$) δ 191.4, 166.5, 162.2, 128.5, 114.3, 109.5, 101.4, 79.8, 55.8, 48.8, 26.9; MS (ESI+) m/z calcd for $C_{12}H_{14}O_3$ $[M + H]^+$ 207.09, found m/z 207.17.

7-Methoxy-2,2-dimethyl-3-methylene-2,3-dihydrochromen-4-one (2). To a solution of **1** (1.0 g, 4.85 mmol) and paraformaldehyde (437 mg, 14.6 mmol) in dioxane (50 mL) was added *N*-methylanilinium trifluoroacetate (2.15 g, 9.7 mmol). The mixture was stirred at 80 °C before the second portion of paraformaldehyde (418 mg, 7.3 mmol) and *N*-methylanilinium trifluoroacetate (1.08 g, 4.9 mmol) were added to the reaction mixture after 5 h. After 5 h of additional stirring, the third portion of the same amounts of paraformaldehyde and *N*-methylanilinium trifluoroacetate was added. After the reaction was complete as monitored by TLC, the reaction mixture was cooled to rt. The reaction mixture was filtered to remove dark brown solid formed during the reaction, and the resulting filtrate was condensed under reduced pressure. The crude mixture was diluted by CH_2Cl_2 and washed with dd H_2O. The aqueous layer was extracted with CH_2Cl_2 three times, and the combined organic layer was dried over anhydrous $MgSO_4$ and filtered. The filtrate was condensed under reduced pressure, and the resulting mixture was purified with silica gel flash column chromatography (diethyl ether/hexanes = 1:12) to provide a desired product **2** (754 mg, 55%) as a light yellow solid: TLC R_f = 0.38 (diethyl ether/hexanes, 1:3); ^{1}H NMR (500 MHz, $CDCl_3$) δ 7.89 (d, J = 9.0 Hz, 1H), 6.58 (dd, J = 9.0, 2.5 Hz, 1H), 6.36 (d, J = 2.5 Hz, 1H), 6.27 (s, 1H), 5.12 (s, 1H), 3.83 (s, 3H), 1.61 (s, 6H); ^{13}C NMR (125 MHz, $CDCl_3$) δ 181.2, 166.6, 162.1, 147.5, 129.6, 120.0, 114.6, 110.3, 101.5, 81.4, 55.8, 27.3; MS (ESI+) m/z calcd for $C_{13}H_{14}O_3$ $[M + H]^+$ 219.09, found m/z 219.19.

3-(Hydroxymethylene)-7-methoxy-2,2-dimethyl-2,3-dihydrochromen-4-one (4). Ethyl formate (1.97 mL, 24.5 mmol) was added to sodium methoxide (1.05 g, 19.4 mmol) suspended in distilled toluene (25 mL) and stirred for 10 min at rt. To the resulting mixture was added compound **1** (1.0 g, 4.9 mmol) in distilled toluene (25 mL) dropwise at 0 °C and stirred for 10 h at rt. After the reaction was complete as monitored by TLC, the reaction mixture was condensed in vacuo and the resultant was diluted by CH_2Cl_2 and washed with brine and satd NH_4Cl (aq). The aqueous layer was extracted with CH_2Cl_2 three times. The combined organic layer was dried over anhydrous $MgSO_4$. The filtrate was condensed under reduced pressure, and the resulting mixture was purified with silica gel flash column chromatography (diethyl ether/hexanes = 1:20) to provide a desired product **4** (677 mg, 59%) as a light yellow solid: TLC R_f = 0.38 (diethyl ether/hexanes, 1:5); ^{1}H NMR (500 MHz, $CDCl_3$) δ 7.79 (d, J = 9.0 Hz, 1H), 7.77 (d, J = 8.5 Hz, 1H), 6.58 (dd, J = 9.0, 2.5 Hz, 1H), 6.36 (d, J = 2.0 Hz, 1H), 3.83 (s, 3H), 1.59 (s, 6H); ^{13}C NMR (125 MHz, $CDCl_3$) δ 179.9, 165.1, 163.9, 158.6, 125.8, 111.4, 110.9, 107.5, 99.1, 76.5, 53.2, 25.9; MS (ESI+) m/z calcd for $C_{13}H_{14}O_4$ $[M + H]^+$ 235.09, found m/z 235.12.

General Procedure: Pyridine Formation Reaction (Hantzsch Condensation), 3a−e. 3-Methylenechromen-4-one **2** (70 mg, 0.321 mmol) and enamine (0.963 mmol) were dissolved in *i*-PrOH (1 mL) and stirred at 105 °C until the solvent was evaporated and neat brown mixture was remained. The resulting product was then heated at 90 °C for 5 h without stirring. Neat mixture was cooled to rt and purified with silica gel flash column chromatography (EtOAc/hexanes = 1:10) without aqueous workup to provide a desired product **3**.

Characterization of compound 3a: yield 84% as a white solid; TLC R_f = 0.48 (EtOAc/hexanes, 1:3); ^{1}H NMR (500 MHz, $CDCl_3$) δ 8.19 (d, J = 8.5 Hz, 1H), 7.96 (s, 1H), 6.64 (dd, J = 8.5, 2.5 Hz, 1H), 6.46 (d, J = 2.5 Hz, 1H), 3.92 (s, 3H), 3.82 (s, 3H), 2.86 (s, 3H), 1.67 (s, 6H); ^{13}C NMR (125 MHz, $CDCl_3$) δ 167.2, 163.6, 159.5, 156.9, 149.5, 133.6, 130.0, 126.8, 122.8, 115.1, 109.2, 102.3, 78.6, 55.6, 52.3, 27.9, 25.3; HRMS (FAB+) calcd for $C_{18}H_{19}NO_4$ $[M + H]^+$ 314.1392, found *m*/*z* 314.1396 (Δ 1.3 ppm).

Characterization of compound 3b: yield 64% as a white solid; TLC R_f = 0.27 (EtOAc/hexanes, 1:10); ^{1}H NMR (500 MHz, $CDCl_3$) δ 8.21 (d, J = 9.0 Hz, 1H), 7.88 (s, 1H), 7.60 (m, 2H), 7.13 (m, 2H), 6.63 (dd, J = 9.0, 2.5 Hz, 1H), 6.48 (d, J = 2.5 Hz, 1H), 3.82 (s, 3H), 3.72 (s, 3H), 1.72 (s, 6H); ^{13}C NMR (125 MHz, $CDCl_3$) δ 168.7, 164.4, 162.5, 163.7, 157.2, 157.0, 149.3, 136.6, 133.6, 131.0, 130.7, 127.0, 124.1, 115.3, 115.2, 114.9, 109.4, 102.2, 78.6, 55.7, 52.5, 27.9; HRMS (FAB+) calcd for $C_{23}H_{20}FNO_4$ $[M + H]^+$ 394.1455, found *m*/*z* 394.1460 (Δ 1.3 ppm).

Characterization of compound 3c: yield 65% as a white solid; TLC R_f = 0.41 (EtOAc/hexanes, 1:5); ^{1}H NMR (500 MHz, $CDCl_3$) δ 8.24 (d, J = 8.5 Hz, 1H), 7.87 (s, 1H), 7.60 (m, 2H), 7.43 (m, 3H), 6.62 (dd, J = 9.0, 2.5 Hz, 1H), 6.48 (d, J = 2.5 Hz, 1H), 4.13 (q, J = 7.0 Hz, 2H), 3.82 (s, 3H), 1.72 (s, 6H), 1.02 (t, J = 7.0 Hz, 3H); ^{13}C NMR (125 MHz, $CDCl_3$) δ 168.7, 163.6, 158.3, 156.9, 149.1, 140.8, 133.3, 130.6, 129.0, 128.7, 128.2, 127.1, 124.9, 115.1, 109.2, 102.2, 78.6, 61.6, 55.7, 27.9, 13.9; HRMS (FAB+) calcd for $C_{24}H_{23}NO_4$ $[M + H]^+$ 390.1705, found *m*/*z* 390.1710 (Δ 1.3 ppm).

Characterization of compound 3d: yield 66% as a white solid; TLC R_f = 0.29 (EtOAc/hexanes, 1:10); ^{1}H NMR (500 MHz, $CDCl_3$) δ 8.20 (d, J = 8.5 Hz, 1H), 7.89 (s, 1H), 7.57 (m, 2H), 7.48 (m, 2H), 6.62 (dd, J = 8.5, 2.5 Hz, 1H), 6.48 (d, J = 2.5 Hz, 1H), 4.17 (q, J = 7.0 Hz, 2H), 3.83 (s, 3H), 1.72 (s, 6H), 1.02 (t, J = 7.0 Hz, 3H); ^{13}C NMR (125 MHz, $CDCl_3$) δ 168.2, 163.7, 157.2, 157.0, 149.3, 139.8, 133.5, 131.3, 131.0, 130.8, 127.0, 124.6, 123.2, 114.9, 109.4, 102.3, 78.7, 61.7, 55.7, 27.9, 14.0; HRMS (FAB+) calcd for $C_{24}H_{22}BrNO_4$ $[M + H]^+$ 468.0810, found *m*/*z* 468.0806 (Δ 1.1 ppm).

Characterization of compound 3e: yield 58% as a white solid; TLC R_f = 0.34 (EtOAc/hexanes, 1:7); ^{1}H NMR (500 MHz, $CDCl_3$) δ 8.21 (d, J = 8.5 Hz, 1H), 7.90 (s, 1H), 6.64 (dd, J = 8.5, 2.5 Hz, 1H), 6.46 (d, J = 2.5 Hz, 1H), 4.38 (q, J = 7.0 Hz, 2H), 3.83 (s, 3H), 3.15 (m, 2H), 1.82 (m, 2H), 1.67 (s, 6H), 1.41(t, J = 7.0 Hz, 3H), 1.03 (t, J = 7.0 Hz, 3H); ^{13}C NMR (125 MHz, $CDCl_3$) δ 167.2 163.4, 162.7, 156.9, 149.2, 133.6, 129.7, 126.8, 123.3, 115.3, 109.2, 102.2, 78.6, 61.4, 55.6, 39.3, 27.9, 23.1, 14.6, 14.5; HRMS (FAB+) calcd for $C_{21}H_{25}NO_4$ $[M + H]^+$ 356.1862, found *m*/*z* 356.1856 (Δ 1.7 ppm).

General Procedure: Pyrazole Formation Reaction, 7a−g. To a stirred mixture of arylhydrazine hydrochloride (0.359 mmol) and triethylamine (0.359 mmol) in ethanol (3 mL) was added 3-hydroxymethylenechromen-4-one **4** (70 mg, 0.299 mmol) and the mixture heated to reflux for 5 h. The resulting yellow solution was condensed in vacuo and diluted by CH_2Cl_2. The reaction mixture was then washed with aqueous citric acid, and the aqueous layer was extracted with CH_2Cl_2 three times. The combined organic layer was dried over $MgSO_4$ and evaporated to give a crude mixture which was purified by silica-gel flash column chromatography (EtOAc/hexanes = 1:7). In condition I, 3-hydroxymethylenechromen-4-one **4** was condensed with arylhydrazines in the neutral salt-free form by the treatment with equal molar amount of triethylamine toward arylhydrazine. In condition II, the identical reaction condition was used for the condensation reaction of **4** with arylhydrazines in the hydrochloride salt form. In condition III, the condensation of **4** with arylhydrazines was pursued in an aqueous acetic acid at 30 °C (acetic acid/H_2O = 2:1).

Characterization of compound 7a: yield 80% as a bright brown solid; TLC R_f = 0.34 (EtOAc/hexanes, 1:3); ^{1}H NMR (500 MHz, $CDCl_3$) δ 7.43 (s, 1H), 7.40 (m, 2H), 7.00(m, 2H), 6.71 (d, J = 8.5 Hz, 1H), 6.56 (d, J = 2.5 Hz, 1H), 6.30 (dd, J = 8.5, 2.5 Hz, 1H), 3.88 (s, 3H), 3.76 (s, 3H), 1.65 (s, 6H); ^{13}C NMR (125 MHz, $CDCl_3$) δ 160.9, 159.9, 154.6, 134.0, 133.8, 133.0, 127.8, 123.3, 121.5, 114.7, 108.9, 107.5, 103.7, 77.8, 55.8, 55.5, 28.9; HRMS (FAB+) calcd for $C_{20}H_{20}N_2O_3$ $[M + H]^+$ 337.1552, found *m*/*z* 337.1551 (Δ 0.3 ppm).

Characterization of compound 7b: yield 87% as a yellow solid; TLC R_f = 0.43 (EtOAc/hexanes, 1:4); ^{1}H NMR (500 MHz, $CDCl_3$) δ 7.44 (s, 1H), 7.37 (d, J = 8.5 Hz, 2H), 7.29(d, J = 8.0 Hz, 2H), 6.75 (d, J = 8.5 Hz, 1H), 6.56 (d, J = 2.5 Hz, 1H), 6.30 (dd, J = 8.5, 2.5 Hz, 1H), 3.76 (s, 3H), 2.45 (s, 3H), 1.65 (s, 6H); ^{13}C NMR (125 MHz, $CDCl_3$) δ 161.0, 154.6, 138.3, 134.2, 132.9, 130.1, 126.2, 123.5, 121.8, 108.9, 107.5, 103.8, 77.8, 55.5, 28.8, 21.5; HRMS (FAB+) calcd for $C_{20}H_{20}N_2O_2$ $[M + H]^+$ 321.1603, found *m*/*z* 321.1612 (Δ 2.8 ppm).

Characterization of compound 7c: yield 77% as a light yellow solid; TLC R_f = 0.47 (EtOAc/hexanes, 1:4); ^{1}H NMR (500 MHz, $CDCl_3$) δ 7.49 (m, 5H), 7.45 (s, 1H), 6.73 (d, J = 9.0 Hz, 1H), 6.56 (d, J = 2.5 Hz, 1H), 6.29 (dd, J = 9.0, 2.5 Hz, 1H), 3.75 (s, 3H), 1.65 (s, 6H); ^{13}C NMR (125 MHz, $CDCl_3$) δ 161.1, 154.6, 140.8, 132.9, 134.4, 129.5, 128.9, 126.4, 123.5, 122.0, 108.8, 107.5, 103.9, 77.7, 55.5, 28.8; HRMS (FAB+) calcd for $C_{19}H_{18}N_2O_2$ $[M + H]^+$ 307.1447, found *m*/*z* 307.1447 (Δ 0.0 ppm).

Characterization of compound 7d: yield 80% as a pale yellow solid; TLC R_f = 0.42 (EtOAc/hexanes, 1:3); ^{1}H NMR (500 MHz, $CDCl_3$) δ 7.50 (m, 2H), 7.46 (s, 1H), 7.20(m, 2H), 6.71 (d, J = 8.5 Hz, 1H), 6.58 (d, J = 3.0 Hz, 1H), 6.33 (dd, J = 8.5, 2.5 Hz, 1H), 3.77 (s, 3H), 1.66 (s, 6H); ^{13}C NMR (125 MHz, $CDCl_3$) δ 163.7, 161.7, 161.2, 154.7, 136.9, 134.5, 133.1, 128.2, 123.2, 122.0, 116.6, 116.4, 108.6, 107.6, 103.9, 77.7, 55.5, 28.8; HRMS (FAB+) calcd for $C_{19}H_{17}FN_2O_2$ $[M + H]^+$ 325.1352, found *m*/*z* 325.1350 (Δ 0.6 ppm).

Characterization of compound 7e: yield 75% as a yellow solid; TLC R_f = 0.34 (EtOAc/hexanes, 1:4); ^{1}H NMR (500 MHz, $CDCl_3$) δ 7.46 (m, 5H), 6.76 (d, J = 8.5 Hz, 1H), 6.57 (d, J = 2.5 Hz, 1H), 6.34 (dd, J = 8.5, 2.5 Hz, 1H), 3.77 (s, 3H), 1.64 (s, 6H); ^{13}C NMR (125 MHz, $CDCl_3$) δ 161.2, 154.7, 139.2, 134,8, 134.6, 133.1, 129.7, 127.5, 123.4, 122.4, 108.5, 107.6, 104.0, 77.7, 55.6, 28.7; HRMS (FAB+) calcd for $C_{19}H_{17}ClN_2O_2$ $[M + H]^+$ 341.1057, found *m*/*z* 341.1055 (Δ 0.6 ppm).

Characterization of compound 7f: yield 88% as a light yellow solid; TLC R_f = 0.52 (EtOAc/hexanes, 1:3); ^{1}H NMR (500 MHz, $CDCl_3$) δ 7.76 (d, J = 8.5 Hz, 2H), 7.66 (d, J = 8.0 Hz, 2H), 7.49 (s, 1H), 6.80 (d, J = 8.5 Hz, 1H), 6.59 (d, J = 2.5 Hz, 1H), 6.36 (dd, J = 8.5, 2.5 Hz, 1H), 3.77 (s, 3H), 1.64 (s, 6H); ^{13}C NMR (125 MHz, $CDCl_3$) δ 161.3, 154.7, 143.5, 135.3, 133.1, 126.7, 126.0, 123.5, 123.1, 108.4, 107.7, 104.1, 77.7, 55.6, 28.5; HRMS (FAB+) calcd for $C_{20}H_{18}F_3N_2O_2$ $[M + H]^+$ 375.1320, found *m*/*z* 375.1324 (Δ 1.1 ppm).

Characterization of compound 7g: yield 84% as a yellow solid; TLC R_f = 0.47 (EtOAc/hexanes, 1:4); ^{1}H NMR (500 MHz, $CDCl_3$) δ 8.36 (d, J = 8.5 Hz, 2H), 7.74 (d, J = 8.5 Hz, 2H), 7.54 (s, 1H), 6.86 (d, J = 8.0 Hz, 1H), 6.61 (d, J = 2.5 Hz, 1H), 6.39 (dd, J = 8.5, 2.5 Hz, 1H), 3.79 (s, 3H), 1.64 (s, 6H); ^{13}C NMR (125 MHz, $CDCl_3$) δ 161.5, 154.7, 147.0, 145.6, 136.1, 133.4, 125.9, 125.0, 123.9, 123.5, 108.2, 107.8, 104.3, 77.7, 55.6, 28.3; HRMS (FAB+) calcd for $C_{19}H_{18}N_3O_4$ $[M + H]^+$ 352.1297, found *m*/*z* 352.1295 (Δ 0.6 ppm).

General Procedure: Pyrazolo[1,5-*a*]pyrimidine Formation Reaction, 9a−e. A mixture of 3-hydroxymethylenechromen-4-one **4** (70 mg, 0.299 mmol) and 3-aminopyrazole (0.299 mmol)

dissolved in glacial acetic acid (1.5 mL) was reacted under microwave irradiation (70 W, 100 °C) for 15 min. The resulting yellow mixture was diluted with CH_2Cl_2 and then neutralized by aqueous $NaHCO_3$. The aqueous layer was extracted with CH_2Cl_2 three times, and the combined organic layer was dried over anhydrous $MgSO_4$. The filtrate was condensed to provide the crude mixture, which was purified by silica-gel flash column chromatography.

Characterization of compound 9a: yield 95% as a bright yellow solid; TLC $R_f = 0.48$ (EtOAc/hexanes, 1:1); ^{1}H NMR (500 MHz, $CDCl_3$) δ 9.41 (d, $J = 8.5$ Hz, 1H), 8.35 (s, 1H), 8.21 (d, $J = 2.0$ Hz, 1H), 6.73 (m, 2H), 6.56 (d, $J = 3.0$ Hz, 1H), 3.86 (s, 3H), 1.76 (s, 6H); ^{13}C NMR (125 MHz, $CDCl_3$) δ 164.2, 157.8, 149.9, 144.9, 144.7, 135.6, 131.7, 117.0, 108.7, 108.4, 103.0, 96.6, 77.1, 55.7, 27.9; HRMS (FAB+) calcd for $C_{16}H_{15}N_3O_2$ $[M + H]^+$ 282.1243, found *m/z* 282.1242 (Δ 0.4 ppm).

Characterization of compound 9b: yield 89% as a bright yellow solid; TLC $R_f = 0.50$ (EtOAc/hexanes, 1:1); ^{1}H NMR (500 MHz, $CDCl_3$) δ 9.31 (d, $J = 9.0$ Hz, 1H), 8.64 (s, 1H), 8.60 (s, 1H), 6.73 (dd, $J = 9.0$, 2.5 Hz, 1H), 6.55 (d, $J = 2.5$ Hz, 1H), 4.46 (q, $J = 7.0$ Hz, 2H), 3.88 (s, 3H), 1.77 (s, 6H), 1.44 (t, $J = 7.0$ Hz, 3H); ^{13}C NMR (125 MHz, $CDCl_3$) δ 164.9, 162.9, 158.3, 148.8, 147.7, 147.6, 136.9, 132.1, 118.7, 109.2, 107.6, 103.0, 102.4, 77.1, 60.5, 55.8, 27.8, 14.8; HRMS (FAB+) calcd for $C_{19}H_{19}N_3O_4$ $[M + H]^+$ 354.1454, found *m/z* 354.1452 (Δ 0.6 ppm).

Characterization of compound 9c: yield 90% as a bright yellow solid; TLC $R_f = 0.42$ (EtOAc/hexanes, 1:1); ^{1}H NMR (500 MHz, $CDCl_3$) δ 9.46 (d, $J = 9.0$ Hz, 1H), 8.28 (s, 1H), 6.74 (dd, $J = 8.5$, 2.5 Hz, 1H), 6.55 (d, $J = 2.5$ Hz, 1H), 6.49 (s, 1H), 3.87 (s, 3H), 2.58 (s, 3H), 1.74 (s, 6H); ^{13}C NMR (125 MHz, $CDCl_3$) δ 164.0, 157.8, 155.2, 150.7, 144.3, 135.0, 131.9, 116.3, 108.6, 108.5, 103.0, 95.7, 77.1, 55.7, 28.0, 15.1; HRMS (FAB+) calcd for $C_{17}H_{17}N_3O_2$ $[M + H]^+$ 296.1399, found *m/z* 296.1398 (Δ 0.3 ppm).

Characterization of compound 9d: yield 96% as a bright yellow solid; TLC $R_f = 0.74$ (EtOAc/hexanes, 1:1); ^{1}H NMR (500 MHz, $CDCl_3$) δ 9.57 (d, $J = 9.0$ Hz, 1H), 8.30 (s, 1H), 8.08 (d, $J = 6.0$ Hz, 2H), 7.48 (t, $J = 9.0$ Hz, 2H), 7.39 (t, $J = 6.0$ Hz, 1H), 6.99 (s, 1H), 6.76 (dd, $J = 9.0$, 2.5 Hz, 1H), 6.55 (d, $J = 2.5$ Hz, 1H), 3.86 (s, 3H), 1.75 (s, 6H); ^{13}C NMR (125 MHz, $CDCl_3$) δ 164.2, 157.9, 156.2, 151.1, 144.7, 135.4, 133.3, 132.0, 131.9, 129.2, 129.0, 126.9, 117.0, 108.7, 108.5, 103.0, 93.2, 93.2, 77.1, 55.7, 28.0; HRMS (FAB+) calcd for $C_{22}H_{19}N_3O_2$ $[M + H]^+$ 358.1556, found *m/z* 358.1557 (Δ 0.3 ppm).

Characterization of compound 9e: yield 95% as a bright yellow solid; TLC $R_f = 0.43$ (EtOAc/hexanes, 1:2); ^{1}H NMR (500 MHz, $CDCl_3$) δ 9.57 (d, $J = 9.0$ Hz, 1H), 8.29 (s, 1H), 8.00 (d, $J = 9.0$ Hz, 2H), 7.01 (d, $J = 8.5$ Hz, 2H), 6.91 (s, 1H), 6.76 (dd, $J = 9.0$, 2.5 Hz, 1H), 6.55 (d, $J = 2.5$ Hz, 1H), 3.86 (s, 3H), 3.87 (s, 3H), 1.75 (s, 6H); ^{13}C NMR (125 MHz, $CDCl_3$) δ 164.1, 160.6, 157.9, 156.1, 151.1, 144.5, 135.2, 132.0, 128.2, 126.0, 116.8, 114.4, 108.7, 108.6, 103.0, 92.4, 77.1, 55.7, 55.6, 28.0; HRMS (FAB+) calcd for $C_{23}H_{21}N_3O_3$ $[M + H]^+$ 388.1661, found *m/z* 388.1660 (Δ 0.3 ppm).

General Procedure: Pyrimidine Formation Reaction, 11a−g. Pyrrolidine (46 μL, 0.555 mmol) was added to 3-hydroxymethylenechromen-4-one **4** (100 mg, 0.427 mmol) in distilled toluene (5 mL) containing 4 Å molecular sieves. The mixture was stirred at rt for 3 h until the color of the reaction mixture turned yellow. After the formation of enaminone **10**, the reaction mixture was transferred to another round-bottom flask, and the remaining molecular sieves were extracted with CH_2Cl_2 five times to recover soaked products. The combined solution was condensed under reduced pressure and redissolved in ethanol (1 mL). To a solution of the resulting mixture were added amidine hydrochloride (1.281 mmol) and sodium hydroxide (0.854 mmol) in ethanol (3 mL). After 5 h of reflux stirring, the reaction mixture was cooled to rt and condensed under reduced pressure. The crude mixture was diluted by CH_2Cl_2 and washed with ddH_2O. The aqueous layer was extracted with CH_2Cl_2 three times, and the combined organic layer was dried over anhydrous $MgSO_4$. The filtrate was condensed under reduced pressure and purified by silica-gel flash column chromatography using EtOAc/hexane as eluents.

Characterization of compound 11a. yield 51% as a white solid; TLC $R_f = 0.80$ (EtOAc/hexanes, 1:1); ^{1}H NMR (500 MHz, $CDCl_3$) δ 8.53 (m, 2H), 8.51 (s, 1H), 7.50 (m, 3H), 6.68 (dd, $J = 8.5$, 2.5 Hz, 1H), 6.47 (d, $J = 2.5$ Hz, 1H), 3.84 (s, 3H), 1.72 (s, 6H); ^{13}C NMR (125 MHz, $CDCl_3$) δ 164.5, 163.9, 157.9, 154.5, 151.7, 138.1, 130.8, 128.7, 128.4, 127.3, 126.9, 113.7, 1109.6, 02.3, 77.7, 55.7, 27.9; HRMS (FAB+) calcd for $C_{20}H_{18}N_2O_2$ $[M + H]^+$ 319.1447, found *m/z* 319.1450 (Δ 0.9 ppm).

Characterization of compound 11b: yield 42% as a white solid; TLC $R_f = 0.77$ (EtOAc/hexanes, 1:1); ^{1}H NMR (500 MHz, $CDCl_3$) δ 8.49 (s, 1H), 8.41 (d, $J = 8.0$ Hz, 2H), 8.33 (d, $J = 8.5$ Hz, 1H) 7.30 (d, $J = 8.0$ Hz, 2H), 6.68 (dd, $J = 8.5$, 2.5 Hz, 1H), 6.47 (d, $J = 2.5$ Hz, 1H), 3.84 (s, 3H), 1.72 (s, 6H); ^{13}C NMR (125 MHz, $CDCl_3$) δ 164.5, 163.9, 157.9, 154.4, 151.6, 141.0, 135.4, 129.5, 128.3, 127.0, 126.9, 113.8, 109.5, 102.2, 77.7, 55.7, 27.9, 21.8; HRMS (FAB+) calcd for $C_{21}H_{20}N_2O_2$ $[M + H]^+$ 333.1603, found 333.1604 (Δ 0.3 ppm).

Characterization of Compound 11c: yield 59% as a white solid; TLC $R_f = 0.78$ (EtOAc/hexanes, 1:1); ^{1}H NMR (500 MHz, $CDCl_3$) δ 8.48 (s, 1H), 8.47 (m, 2H), 8.29 (d, $J = 9.0$ Hz, 1H), 7.46 (m, 2H), 6.68 (dd, $J = 9.0$, 2.5 Hz, 1H), 6.47 (d, $J = 2.5$ Hz, 1H), 3.85 (s, 3H), 1.72 (s, 6H); ^{13}C NMR (125 MHz, $CDCl_3$) δ 164.6, 162.9, 157.9, 154.6, 151.7, 136.9, 136.6, 129.7, 128.9, 127.4, 126.9, 113.6, 109.6, 102.3, 77.7, 55.7, 27.9; HRMS (FAB+) calcd for $C_{20}H_{17}ClN_2O_2$ $[M + H]^+$ 353.1057, found 353.1066 (Δ 2.5 ppm).

Characterization of compound 11d: yield 56% as a white solid; TLC $R_f = 0.63$ (EtOAc/hexanes, 1:1); ^{1}H NMR (500 MHz, $CDCl_3$) δ 8.49 (m, 2H), 8.46 (s, 1H), 8.31 (d, $J = 9.0$ Hz, 1H), 7.26 (s, 1H), 6.99 (m, 2H), 6.67 (dd, $J = 9.0$, 2.5 Hz, 1H), 6.46 (d, $J = 2.5$ Hz, 1H), 3.88 (s, 3H), 3.84 (s, 3H), 1.71 (s, 6H); ^{13}C NMR (125 MHz, $CDCl_3$) δ 164.4, 163.6, 162.0, 157.9, 154.3, 151.6, 130.8, 129.9, 126.8, 126.6, 114.0, 113.8, 109.5, 102.3, 77.6, 55.7, 55.6, 27.9; HRMS (FAB+) calcd for $C_{21}H_{20}N_2O_3$ $[M + H]^+$ 349.1552, found 349.1547 (Δ 1.4 ppm).

Characterization of compound 11e: yield 47% as a pale yellow solid; TLC $R_f = 0.51$ (EtOAc/hexanes, 1:1); ^{1}H NMR (500 MHz, $CDCl_3$) δ 8.33 (s, 1H), 8.15 (d, $J = 8.5$ Hz, 1H), 6.64 (dd, $J = 8.5$, 2.5 Hz, 1H), 6.45 (d, $J = 2.5$ Hz, 1H), 3.84 (s, 3H), 2.72 (s, 3H), 1.68 (s, 6H); ^{13}C NMR (125 MHz, $CDCl_3$) δ 167.5, 164.5, 157.8, 154.4, 151.3, 126.7, 126.4, 113.6, 109.5, 102.3, 55.7, 27.8, 26.3; HRMS (FAB+) calcd for $C_{15}H_{16}N_2O_2$ $[M + H]^+$ 257.1290, found 257.1289 (Δ 0.4 ppm).

Characterization of compound 11f: yield 47% as a white solid; TLC $R_f = 0.20$ (EtOAc/hexanes, 1:1); ^{1}H NMR (500 MHz, $CDCl_3$) δ 8.05 (s, 1H), 8.02 (d, $J = 8.5$ Hz, 1H), 6.60 (dd, $J = 8.5$, 2.5 Hz, 1H), 6.43 (d, $J = 2.5$ Hz, 1H), 5.31 (s, 2H), 3.82 (s, 3H), 1.63 (s, 6H); ^{13}C NMR (125 MHz, $CDCl_3$) δ 164.2, 162.8, 158.0, 155.6, 152.6, 126.5, 120.7, 113.6, 109.2, 102.2, 77.7, 55.7, 28.1; HRMS (FAB+) calcd for $C_{14}H_{15}N_3O_2$ $[M + H]^+$ 258.1243, found 258.1241 (Δ 0.8 ppm).

Characterization of compound 11g: yield 49% as a white solid; TLC $R_f = 0.70$ (EtOAc/hexanes, 1:1); ^{1}H NMR (500 MHz, $CDCl_3$) δ 8.40 (s, 1H), 8.21 (d, $J = 8.5$ Hz, 1H), 6.64 (dd, $J = 8.5$, 2.5 Hz, 1H), 6.45 (d, $J = 2.5$ Hz, 1H), 3.83 (s, 3H), 1.68 (s, 6H), 1.45 (s, 9H); ^{13}C NMR (125 MHz, $CDCl_3$) δ 176.5, 164.2, 157.7, 153.6, 151.0, 126.7, 126.0, 114.0, 109.4, 102.2, 77.6, 55.7, 39.6, 29.9, 27.9; HRMS (FAB+) calcd for $C_{18}H_{22}N_2O_2$ $[M + H]^+$ 299.1760, found 299.1754 (Δ 2.0 ppm).

Acknowledgment. This work is supported by Grant No. R15-2006-020 from the National Core Research Center (NCRC) program of the Ministry of Science & Technology (MOST) and the Korea Science and Engineering Foundation (KOSEF) through the Center for Cell Signaling & Drug Discovery Research at Ewha Womans University, MarineBio21, Ministry of Maritime

Affairs and Fisheries, Korea (MOMAF), and the Molecular and Cellular BioDiscovery Research Program from MOST. H.A. and M.K. are grateful for the award of a BK21 fellowship.

Supporting Information Available: General experimental procedures, structural confirmation of each core skeleton (I−IV), as well as ^{1}H NMR and ^{13}C NMR spectra and mass spectra for all new compounds. Crude ^{1}H NMR spectra for typical patterns of regioisomers in pyrazole synthesis. Data from computational studies including principle component analysis loading data, conformer alignment, and isosurface diagrams. This material is available free of charge via the Internet at http://pubs.acs.org.

JO702196F